A role for trypanosomatid aldo-keto reductases in methylglyoxal, prostaglandin and isoprostane metabolism

Roberts, Adam; Dunne, Joanne; Scullion, Stanley; Norval, Suzanne; Fairlamb, Alan

Published in:
Biochemical Journal

DOI:
10.1042/BCJ20180232

Publication date:
2018

Document Version
Publisher's PDF, also known as Version of record

Biochemical Journal (2018) **475** 2593–2610
https://doi.org/10.1042/BCJ20180232

PORTLAND PRESS

Research Article

A role for trypanosomatid aldo-keto reductases in methylglyoxal, prostaglandin and isoprostane metabolism

Adam J. Roberts*, Joanne Dunne†, Paul Scullion, Suzanne Norval and Alan H. Fairlamb

Division of Biological Chemistry and Drug Discovery, School of Life Sciences, University of Dundee, Dundee DD1 5EH, U.K.

Correspondence: Alan H. Fairlamb (a.h.fairlamb@dundee.ac.uk)

OPEN ACCESS

Trypanosomatid parasites are the infectious agents causing Chagas disease, visceral and cutaneous leishmaniasis and human African trypanosomiasis. Recent work of others has implicated an aldo-keto reductase (AKR) in the susceptibility and resistance of *Trypanosoma cruzi* to benznidazole, a drug used to treat Chagas disease. Here, we show that *Tc*AKR and homologues in the related parasites *Trypanosoma brucei* and *Leishmania donovani* do not reductively activate monocyclic (benznidazole, nifurtimox and fexinidazole) or bicyclic nitro-drugs such as PA-824. Rather, these enzymes metabolise a variety of toxic ketoaldehydes, such as glyoxal and methylglyoxal, suggesting a role in cellular defence against chemical stress. UPLC-QToF/MS analysis of benznidazole bioactivation by *T. cruzi* cell lysates confirms previous reports identifying numerous drug metabolites, including a dihydro-dihydroxy intermediate that can dissociate to form *N*-benzyl-2-guanidinoacetamide and glyoxal, a toxic DNA-glycating and cross-linking agent. Thus, we propose that *Tc*AKR contributes to benznidazole resistance by the removal of toxic glyoxal. In addition, three of the four enzymes studied here display activity as prostaglandin $F_{2\alpha}$ synthases, despite the fact that there are no credible cyclooxygenases in these parasites to account for formation of the precursor PGH_2 from arachidonic acid. Our studies suggest that arachidonic acid is first converted non-enzymatically in parasite lysates to (PGH_2-like) regioisomers by free radical-mediated peroxidation and that AKRs convert these lipid peroxides into isoprostanes, including prostaglandin $F_{2\alpha}$ and 8-iso-prostaglandin $F_{2\alpha}$.

Introduction

Parasitic protozoa belonging to the order Kinetoplastida cause three neglected tropical diseases, Chagas disease, human African trypanosomiasis and leishmaniasis due to infection with *Trypanosoma cruzi*, *Trypanosoma brucei* and *Leishmania* spp., respectively, see review [1]. The burden of these three 'neglected' tropical diseases is almost exclusively associated with poverty and therefore there has been little incentive for pharmaceutical companies to invest in developing new treatments, see review [2]. Currently, the nitro-drugs benznidazole and nifurtimox developed over 40 years ago are the only therapies available for the treatment of Chagas disease, with nifurtimox also constituting part of the combination therapy 'NECT' for late-stage human African trypanosomiasis [3]. In addition, another nitro-drug, fexinidazole, has shown activity against all three parasites [4–6] and consequentially is now under clinical assessment for all three diseases.

The anti-parasitic activities of these nitro-containing pro-drugs are dependent upon parasite-facilitated bio-activation by a bacterial-like type I nitroreductase NTR1 [7] to form toxic reactive intermediates [8–10], and consequently, loss of NTR1 is a key resistance determinant [11,12]. Notably, other enzymes have been implicated in resistance to benznidazole in *T. cruzi*, the FMN containing 'old yellow enzyme' a functional prostaglandin $F_{2\alpha}$ synthase [13,14] and an aldo-keto reductase (AKR)

*Present address: Cell Surface Signalling Laboratory, Welcome Trust Sanger Institute, Cambridge CB10 1SA, U.K.
†Present address: School of Chemistry, Joseph Black Building, West Mains Road, University of Edinburgh, Edinburgh EH9 3JJ, U.K.

Received: 19 March 2018
Revised: 10 July 2018
Accepted: 16 July 2018

Accepted Manuscript online: 25 July 2018
Version of Record published: 29 August 2018

Biochemical Journal (2018) **475** 2593–2610
https://doi.org/10.1042/BCJ20180232

Table 1 List of primers used in the present study

Primer	Sequence
*Tc*AKR-F	catATGAATTGCAATTACAACTGTGTGACACTCC
*Tc*AKR-R	ggatccTCACTCCTCTCCACCAGGG
*Tb*PGFS-F	catATGGCTCTCACTCAATCCCTAAAACTC
*Tb*PGFS-R	ggatccTCAAAAGTCGTTCATGAAGACCTCC
*Li*PGFS2-F	aaaacatATGGCTGACGTTGGTAAGGCAATGG
*Li*PGFS2-R	ttttggatccTTAGAACTGCGCCTCATCGGGGTC
*Tc*PGF2α-F	catATGGCGACGTTCCCCGAAC
*Tc*PGF2α-R	ggatccTTAGTTGTTGTACGTCGGGTAATCG

Restriction sites are underlined.

[15]. Somewhat paradoxically, the latter enzyme has been reported to activate benznidazole, yet overexpression of AKR in *T. cruzi* decreased rather than increased susceptibility to benznidazole [16]. Members of this AKR superfamily, characterised by their ability to reduce aldehydes and/or ketones, have been identified in all domains of life [17]. The activity of these enzymes requires either NADH and/or NADPH to reduce a variety of substrates, including, but not limited to aldoses, steroids, methylglyoxal [18] or prostaglandins [19]. In the trypanosomatid parasites *Leishmania* spp. and *T. brucei*, the production of prostaglandin $F_{2\alpha}$ has been reported to be catalysed by a member of the AKR family [19,20]; however, the equivalent enzyme in *T. cruzi* is reported not to catalyse this reaction [21]. Given the conflicting and contradictory reports in the literature, we have re-examined the ability of TcAKR to metabolise benznidazole and carried out a comparative enzymological study of trypanosomatid AKRs to elucidate their potential metabolic roles in prostanoid and glyoxal metabolism.

Experimental procedures

Cloning and expression of recombinant proteins

The open reading frames (ORFs) encoding *LiPGFS1* (LinJ.32.0470, http://tritrypdb.org) and *Hs*PGFS (NP_003730.4) were synthesised by GeneART™. The ORFs of *TcAKR* (GenBank MH593394), *TbPGFS* (Tb927.11.4700) and *LiPGF2* (LinJ.31.2210) were amplified from genomic DNA isolated from *T. cruzi* Silvio X10/7 clone A1, *T. brucei* 427 and *Leishmania infantum* genomic DNA, respectively, using primers (Table 1) and pfu polymerase. The resulting PCR products were cloned into TOPO zero blunt. The ORFs of each gene were digested with the appropriate restriction endonucleases and ligated into pET15b-TEV, yielding pET15b-TEV-*HsPGFS*, pET15b-TEV-*TcAKR*, pET15b-TEV-*LiPGFS*1, pET15b-TEV-*LiPGFS*2 and pET15b-TEV-*LiAKR*. All plasmids were sequenced (www.dnaseq.co.uk) to verify the correct sequences.

Plasmids were transformed into Rosetta (DE3) pLysS and 10-ml cultures were used to inoculate 1 l of Autoinduction medium [22] with shaking at 30°C for 12 h. Cells were harvested by centrifugation (5090×***g*** for 30 min at 4°C) and resuspended in buffer A (25 mM sodium phosphate buffer, 300 mM NaCl and 25 mM imidazole, pH 8.0) supplemented with DNase I, lysozyme and complete EDTA-free protease inhibitor cocktail tablets (Roche). Cells were lysed at 30 kPsi using a continuous flow cell disruptor (Constant systems) and soluble proteins obtained by centrifugation (20 000×***g***, 30 min and 4°C). The soluble fraction was loaded onto a 5-ml HisTrap HP column and the bound protein eluted with a gradient of imidazole (0–250 mM) in buffer A. Fractions containing the protein of interest were pooled and the hexahistidine tag was removed with TEV protease overnight at 4°C while dialysing against 25 mM sodium phosphate, 300 mM NaCl, pH 8.0, in a 10 000 MWCO membrane. Pure protein was observed after a final HisTrap HP purification step.

Oligomeric structure

Recombinant proteins were loaded onto a Superdex 75 10/300 or Superose 12 10/300 column, equilibrated in 25 mM HEPES, 150 mM NaCl, pH 7.33 and the elution volume of the recombinant proteins was compared with

that of known protein standards (Bio-Rad). *Tc*AKR separations were also repeated using the Superose 12 10/300 column with the high salt buffer (150 mM Tris–HCl, pH 7.6, 300 mM NaCl) as previously described [21].

Enzyme assays

Enzymatic activity was assessed by measuring the continuous oxidation of NADPH at 340 nm in the presence of varying concentrations of substrate using a Shimadzu UV-2401 or 1601 spectrophotometer. Measurements were taken under steady-state conditions, with a fixed concentration of NADPH (100 μM) in 25 mM HEPES, 150 mM NaCl, pH 7.33, using an appropriate amount of enzyme. Enzyme concentrations for measuring the specific activities were quantified with the Bradford protein assay using bovine serum albumin as standard. Enzyme concentration for kinetic characterisation was determined by UV spectroscopy using the molar extinction coefficients of 37 735 for *Hs*PGFS, 60 470 for *Tc*AKR, 51 590 for *Tb*PGFS, 52 930 for *Li*PGFS1 and 51 530 for *Li*PGFS2 calculated using CLC workbench version 6.9.1. The observed rate of change at 340 nm was converted into s^{-1} prior to fitting the data to the Michaelis–Menten kinetics equation in GraFit 5.0 yielding apparent values for k_{cat} and K_m. Reported values for K_m (K_m^{app}) and k_{cat} values are the weighted mean of independent experiments. Weighted means and standard deviations were calculated using the following equations [23], where A, B…I are the means and a, b…i are standard deviations of A, B, etc.

Weighted mean of individual mean values

$$= \frac{(A/a^2) + (B/b^2) + \ldots + (I/i^2)}{(1/a^2) + (1/b^2) + \ldots + (1/i^2)}$$

Weighted mean of standard deviations

$$= \frac{(1/a) + (1/b) + \ldots + (1/i)}{(1/a^2) + (1/b^2) + \ldots + (1/i^2)}$$

Recombinant prostaglandin $F_{2\alpha}$ synthase assay

A total of 1 mg of purified proteins (*Tc*AKR, *Li*PGFS1, *Li*PGFS2, *Tb*PGFS, *Hs*PGFS and *Tc*OYE) were incubated in the enzyme assay buffer in the presence of 10 μM prostaglandin H2 (Cayman Chemicals) and 100 μM NADPH for 1 h at 37°C. Samples were inactivated by the addition of two volumes of acetonitrile and analysed by LC–MS/MS as described below for the analysis of arachidonic acid and a prostaglandin standard mixture (Cayman Chemicals).

UPLC-QToF/MS analysis of benznidazole metabolism

Recombinant *Tc*AKR (13 μg and 130 μg ml^{-1}) was incubated with 100 μM benznidazole and 100 μM NADPH for 1 h at 37°C in 25 mM HEPES, 150 mM NaCl, pH 7.33. Hypotonic lysates (40 mg) made from *T. cruzi* wild-type or NTR1-overexpressing epimastigotes were incubated with 100 μM benznidazole and 1 mM NADH as described above as a positive control. Reactions with pure enzyme or crude parasite lysates were terminated by the addition of two volumes of acetonitrile and analysed by UPLC-QToF/MS. Metabolite identification samples were analysed on a Waters Acquity UPLC coupled to a Waters Xevo QToF mass spectrometer. Chromatographic separation was achieved on a Waters BEH C18 column (50 × 2.1 mm, 1.7 μm particle size) eluted with A: water + 0.1% formic acid, B: acetonitrile + 0.1% formic acid. A flow rate of 0.5 ml min^{-1} and an injection volume of 5 μl were selected. Analysis was performed with a 7 min LC run: 98% A initially, to 65% A after 4 min then 5% A after 5 min, held for 0.99 min before returning to 98% A after 6 min. MS^E spectra were acquired, allowing exact mass precursor and fragment data to be simultaneously collected over a mass range of 50–1200 m/z with the following mass spectrometer parameters: positive electrospray ionisation, cone voltage 38 V, mass range 100–1200 m/z, ramping collision energy 20–40 V, capillary voltage 1.5 kV, desolvation temperature 500°C, source temperature 120°C, desolvation gas (nitrogen) 800 l h^{-1} and cone gas (nitrogen) 10 l h^{-1}.

Biochemical Journal (2018) 475 2593–2610
https://doi.org/10.1042/BCJ20180232

Table 2 MRM transitions used for detecting the prostaglandin species and their retention times
Chromatograms of the 10 min chromatographic separations are provided in Supplementary Figure S1.

Prostaglandin	MRM transition	Retention time (min)
6-keto $PGF_{1\alpha}$	369.2 > 163.1	3.09
Iso-$PGF_{2\alpha}$	353.0 > 192.9	4.25
$PGF_{2\alpha}$	353.0 > 192.9	4.88
$PGF_{1\alpha}$	355.2 > 311.2	4.96
PGE_2	351.1 > 271.1	5.06
PGE_1	353.2 > 317.2	5.31

Parasite growth and electroporation

Epimastigotes of the *T. cruzi* strain Silvio X10/7 (MHOM/BR/78/Silvio; clone X10/7) clone A1 were grown RTH/FCS medium at 28°C [24]. *T. brucei* bloodstream-form parasites were grown in an HMI9-T [25] medium at 37°C and *Leishmania donovani* (MHOM/SD/62/1S-CL2D) promastigotes were grown in a modified M199 medium described previously [26]. Transgenic parasites overexpressing NTR1 (TCSYLVIO_001958) were generated by transfection of plasmid pTREX-TcNTR1 with an Amaxa Nucleofector 2b device using program U-33. Transgenic parasites were selected by the addition of G418 at 250 μg ml^{-1}.

Arachidonic acid co-culture experiment

T. brucei bloodstream-form parasites, *Leishmania donovani* promastigotes and *T. cruzi* epimastigotes, were incubated in the presence of 66 μM arachidonic acid (Sigma–Aldrich) for 16 h at 37°C, 28°C and 28°C, respectively. Parasites were collected by centrifugation and washed in PBS three times prior to biological inactivation by three rounds of freeze–thaw before mixing with two volumes of acetonitrile and analysis by LC–MS/MS.

Lysate arachidonic acid experiment

T. cruzi epimastigotes and *T. brucei* BSF were harvested by centrifugation at 800×***g*** and washed three times in ice cold PBS. Parasites (1×10^8) were collected and lysed by hypotonic lysis (10 mM Tris–HCl, pH 7.5) for 5 min on ice. Incubations with and without 1 mM arachidonic acid were carried as previously described [19], in a reaction volume of 400 μl and reactions terminated by the addition of 800 μl acetonitrile. Samples were subjected to three rounds of freeze–thaw treatment to ensure biological inactivation, prior to analysis by LC–MS/MS. All samples were analysed on a Waters TQ-S with Acquity UPLC using a Waters BEH C18 column (50 × 2 mm, 1.7 μm particle size). Source temperature was 150°C and desolvation gas temperature was 600°C. Eluents used were A: water + 0.01% formic acid, B: acetonitrile + 0.01% formic acid and the flow rate was 0.5 ml min^{-1}. Initial work on the incubation of arachidonic acid with parasites was performed with a 6 min LC run: 95% A initially, to 80% A after 1 min then 60% A after 4 min, to 5% A after 4.5 min, held for 0.5 min before returning to 95% A after 5.1 min. Further work on the incubation of arachidonic acid with cell lysates was performed with a 10 min LC run: 95% A initially, to 80% A after 1 min then 60% A after 8 min, to 5% A after 8.1 min, held for 0.9 min before returning to 95% A after 9.1 min. Multiple reaction monitoring (MRM) transitions used for the prostaglandin species monitored are listed in Table 2 and Supplementary Figure S1 (all in negative ion mode).

Results

Characterisation of TcAKR

The enzymatic function of *Tc*AKR is far from clear: it is annotated as a prostaglandin F synthase in some genomic databases, yet the recombinant protein is reported to lack such activity [21] and other possible physiological substrates have not been tested. It has also been proposed that *Tc*AKR plays a role in the metabolism of, and resistance to, benznidazole [15,16]. To clarify these issues, *Tc*AKR was expressed in *Escherichia coli*, purified to homogeneity (Figure 1A) and its physico-chemical properties were determined. The purified protein (with or without the His_6-tag) was analysed by size exclusion chromatography and found to elute as a single symmetrical peak with a calculated M_r close to that of a theoretical monomer (Figure 1B), when separated

Biochemical Journal (2018) **475** 2593–2610
https://doi.org/10.1042/BCJ20180232

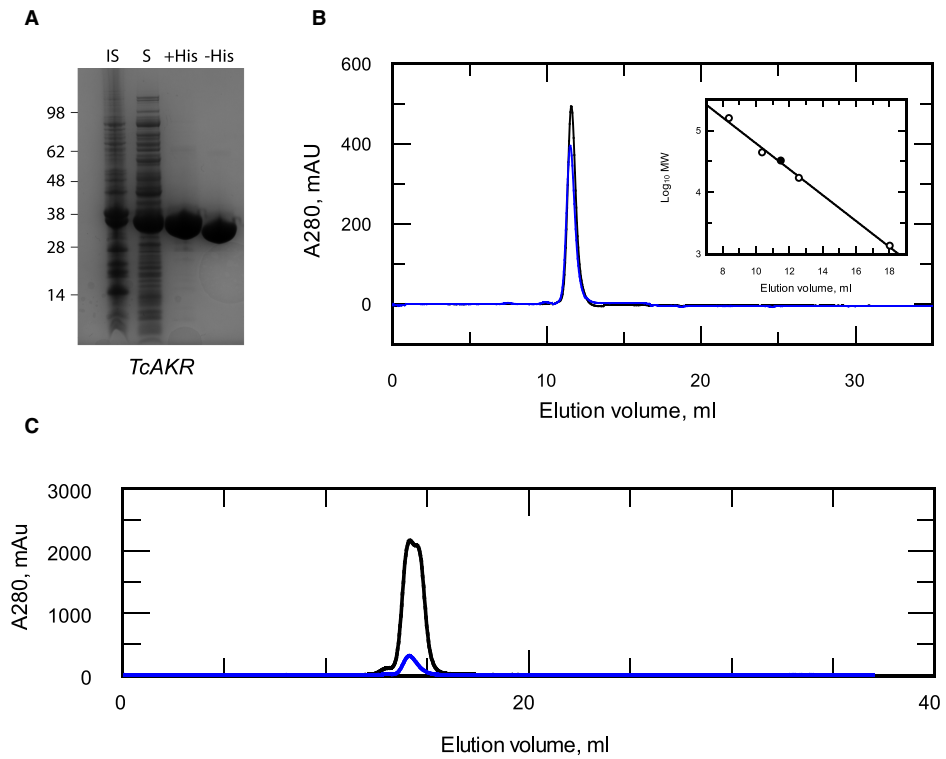

Figure 1. Characterisation of recombinant *Tc*AKR.

(**A**) Purity of recombinant enzyme by SDS–PAGE: insoluble (lane 1), soluble (lane 2), pooled fraction after HisTrap (lane 3) and pooled protein after hexahistidine tag removal (lane 4). (**B**) Elution profile of recombinant *Tc*AKR (black) and His_6-*Tc*AKR (blue) under quasi-physiological conditions from a Superdex 75 10/300 column. (Inset) Elution volumes of known protein standards (open circles) plotted against the $\log_{10}$ of their molecular masses. Theoretical elution volume of the *T. cruzi* AKR monomer (closed circle). Linear fit R^2: 0.998. (**C**) Elution profile of recombinant *Tc*AKR at 2 mg ml^{-1} (black) and 20 mg ml^{-1} (blue) under quasi-physiological conditions from a Superose12 10/300 column.

under quasi-physiological conditions (pH 7.33, 150 mM NaCl). This finding is in complete contrast with that of a previous study by Garavaglia et al. [21], who reported the presence of mixed species containing monomeric, dimeric and tetrameric forms of the enzyme from the CL-Brener strain of *T. cruzi*. When repeating these authors' conditions using the same column and buffer conditions, the *Tc*AKR isolated from our laboratory strain of *T. cruzi* continued to elute as a monomeric species, irrespective of the amount loaded (Figure 1C). The reason for this discrepancy is not clear. Both enzymes are highly similar (97% amino acid sequence identity); however, modelling onto the published crystal structure of this enzyme [27] suggests that the majority of these differences are located on the surface. Notably, one allele in the CL-Brener strain contains an additional cysteine (Y51C) (SNP: NGS_SNP.TcChr40-P.486408), which is absent in the Silvio X10-7 clone used in our study. Modelling on the *Tc*AKR crystal structure 4GIE [27] suggests that this cysteine residue is likely to be solvent accessible and therefore available for disulfide formation with another monomer. This could account for dimer (but not the tetramer) species reported by Garavaglia et al. [21] and would explain why their dimeric species did not dissociate into monomers during mass spectrometry.

Substrate-specificity of TcAKR

As *Tc*AKR has no clear biological role, a BLAST analysis was carried out in an attempt to assign a possible function for this enzyme, identifying enzymes in vitamin K biosynthesis, glyoxal metabolism and synthesis of prostaglandin $F_{2\alpha}$. The activity of *Tc*AKR was assessed with a fixed concentration of a variety of biologically relevant or typical AKR substrates (Table 3) identifying methylglyoxal, a toxic by-product of glycolysis, to have one of the highest specific activities with the purified enzyme. Subsequent characterisation of glyoxal and

Biochemical Journal (2018) **475** 2593–2610
https://doi.org/10.1042/BCJ20180232

Table 3 A survey of purified recombinant trypanosomatid aldo-keto reductases with various substrates

Compounds (60 μM) were assayed spectrophotometrically in the presence of 100 μM NADPH. Specific activity is given in μmol min^{-1} mg^{-1}. Values are the means and standard deviations ($n = 3$).

Substrate	*Tc*AKR	*Li*PGFS1	*Li*PGFS2	*Tb*PGFS
2-Nitrobenzaldehyde	0.20 ± 0.004	1.40 ± 0.04	2.51 ± 0.029	0.73 ± 0.017
3-Nitrobenzaldehyde	0.16 ± 0.003	0.06 ± 0.002	2.40 ± 0.037	1.86 ± 0.009
4-Nitrobenzaldehyde	0.39 ± 0.009	0.06 ± 0.002	2.49 ± 0.142	0.71 ± 0.013
Glyoxal	0.001 ± 0.001	0.02 ± 0.001	0.09 ± 0.001	0.15 ± 0.005
Methylglyoxal	1.20 ± 0.022	0.61 ± 0.02	1.79 ± 0.009	0.67 ± 0.012
Phenylglyoxal	3.66 ± 0.092	3.11 ± 0.018	2.46 ± 0.084	0.78 ± 0.037
Vitamin K3 epoxide	N.A.	N.A.	N.D.	N.A.
Glyceraldehyde	0.05 ± 0.005	N.D.	0.16 ± 0.002	0.13 ± 0.004
Benznidazole	N.A.	N.A.	N.A.	N.A.

Abbreviations: NA, not active; ND, not determined.

methylglyoxal showed them to follow Michaelis–Menten kinetics (Figure 2A,B). Notably, methylglyoxal had a K_m of 0.24 mM and k_{cat}/K_m (1.95×10^4 M s^{-1}) which is similar to that of SakRI (1.1×10^4 M^{-1} s^{-1}), a cyanobacterial enzyme involved in methylglyoxal detoxification [18].

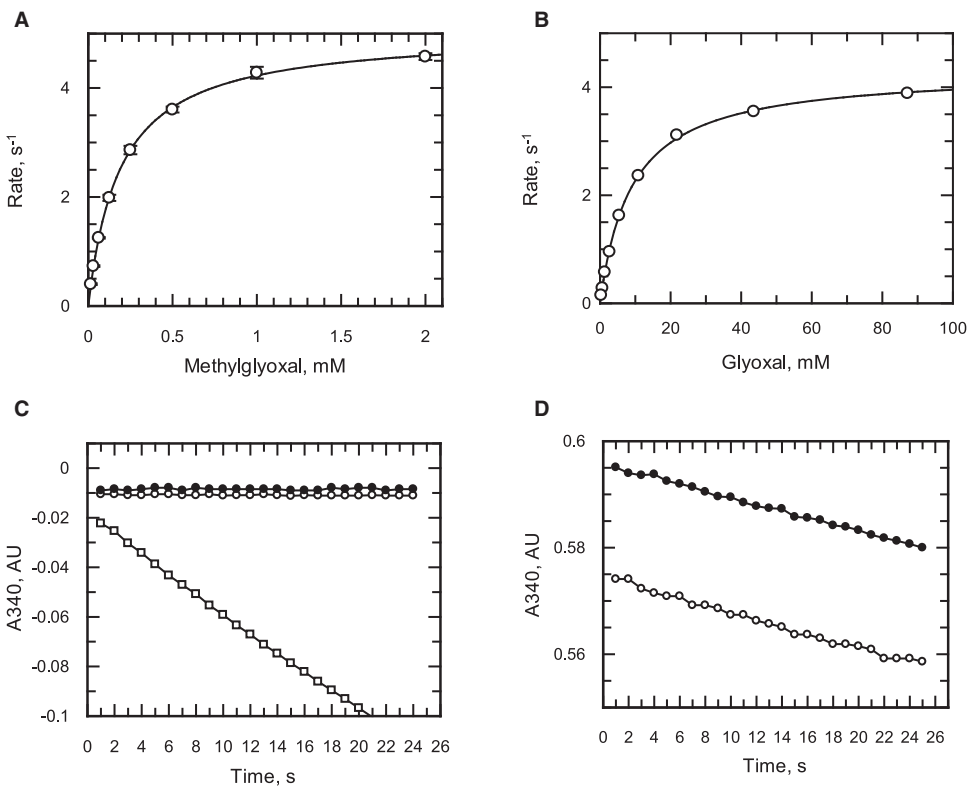

Figure 2. Testing benznidazole as a substrate or inhibitor of recombinant *Tc*AKR.

(**A**) Benznidazole as a substrate of TcAKR, DMSO (open circles), 60 μM benznidazole (closed circles), 60 μM phenylglyoxal (open squares). (**B**) Inhibition of phenylglyoxal (60 μM) metabolism by benznidazole, DMSO (closed circles), 60 μM benznidazole (open circles). (**C** and **D**) Michaelis–Menten plots of activity with glyoxal and methylglyoxal, respectively.

Although benznidazole was recently reported to be a substrate of this enzyme (73 mU mg^{-1}) [16], we were unable to detect any increase in NADPH oxidation above the background rate (1 mU mg^{-1}) when benznidazole was present at 60 μM (Figure 2C). Neither did we observe any inhibition of enzymatic activity by benznidazole with phenylglyoxal as a substrate (Figure 2D). To confirm our negative findings with the spectrophotometric assay, the purified enzyme was incubated with NADPH in the presence or absence of benznidazole for 1 h at 37°C and subsequently analysed by UPLC-QToF/MS. Even in the presence of excess enzyme (130 μg ml^{-1}), we were unable to detect any utilisation of benznidazole (Figure 3A,B). In contrast, incubation of benznidazole with parasite lysates under identical conditions converted more than half of the benznidazole (Figure 3C,D) into multiple metabolites already reported in the literature (Table 4) [8,10]. The smaller peak size of benznidazole incubated with the lysate prepared from NTR-overexpressing parasites (Figure 3D) is consistent with NTR-activating benznidazole [8]. Other clinically pertinent nitro-drugs for the trypanosomatid parasites, nifurtimox, fexinidazole [5] and (*R*)-PA824 [28] were also not substrates for AKR. These results demonstrate that *Tc*AKR is not directly involved with the bio-activation of benznidazole or other nitro-drugs.

Identifying alternative methylglyoxal-reducing enzymes in the trypanosomatids

Homologues of *Tc*AKR were identified in the related parasites *T. brucei* and *L. infantum*, identifying one and two homologues, respectively. The identification of a *T. brucei* homologue was of particular interest as this parasite notably lacks the trypanothione-dependent glyoxalase pathway present in *Leishmania* and *T. cruzi* [29]. The genes encoding these enzymes have been annotated as prostaglandin F synthases, with the *L. infantum* (LinJ.31.2210) and *T. brucei* (Tb927.11.4700) sequences previously assigned to AKR sub-family 5A [17]. Alignments revealed the trypanosomatid sequences to share between 54 and 57% identity with each other (Figure 4) with all maintaining the conserved AKR catalytic tetrad identified in *T. brucei* [30]. To further characterise the enzymatic properties of these proteins, the homologues identified from *T. brucei* and *L. infantum* were overexpressed in *E. coli* and purified to homogeneity using the same two-stage purification as for *Tc*AKR (Figure 5A). The typical yields of pure protein ranged between 10 and 30 mg l^{-1} of starting culture. Similar to *Tc*AKR, the homologues *Tb*PGFS, *Li*PGFS1 and *Li*PGFS2 were primarily monomeric (Figure 5B–D) when analysed by size exclusion chromatography under the same quasi-physiological conditions. However, when *Li*PGFS1 was incubated for 96 h at 4°C in the absence of a reducing agent, 25% of the protein eluted with an apparent mass of a dimer (Figure 5E). The addition of a reducing agent completely abolished the dimeric species (Figure 5E), indicating the dimeric form to be reliant upon disulfide bond formation.

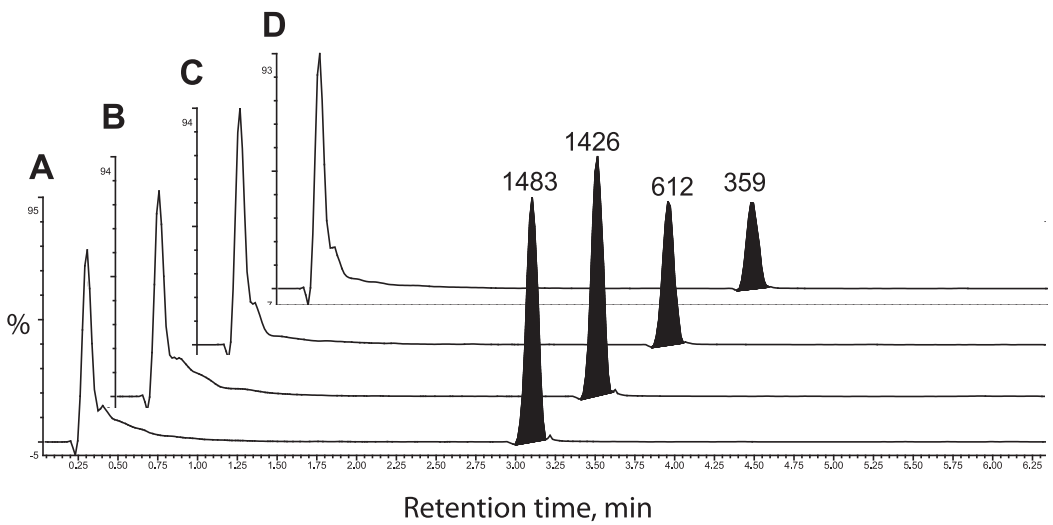

Figure 3. Metabolism of benznidazole by TcAKR and whole cell lysates of *T. cruzi*.

Extracted ion chromatograms measuring the relative amount of benznidazole in the presence of NADH plus (**A**) no enzyme, (**B**) 0.13 mg ml^{-1} recombinant *Tc*AKR, (**C**) 40 mg ml^{-1} of a wild-type *T. cruzi* lysate and (**D**) 40 mg ml^{-1} of a lysate-overexpressing NTR.

Biochemical Journal (2018) 475 2593–2610
https://doi.org/10.1042/BCJ20180232

Table 4 Benznidazole-derived metabolites

Metabolites were identified by accurate mass and presence in the sample, but absence in the control incubations.

Retention time (min)	Structure	Metabolite number[1]	[M +H]$^+$	Ionisation state	WT lysate	NTR^{OE} Lys B	Control	TcAKR
3.1	Benznidazole	NA	261.10	1	NA	NA	NA	NA
1.59	Hydroxylamine or hydroxy derivative 1 or 2	11 or 19	247.11	1	Y	Y	N	N
1.8	Amino derivative of benznidazole	1	231.12	1	Y	Y	N	N
1.49/1.59	Dihydroxy-dihydro derivative	3	265.13	1	Y	Y	N	N
1.59	*N*-benzyl-2-guanidinoacetamide	5	207.13	1	N	Y	N	N
1.3	2-Amino-*N*-benzylacetamide	22	165.10	1	Y	Y	N	N
1.74	Amino derivative + glutathione (isomer 1)	7 or 8	536.19	1	Y	Y	N	N
			268.56	2	Y	Y	N	N
1.83	Amino derivative + glutathione (isomer 2)	7 or 8	536.19	1	Y	Y	N	N
			268.56	2	Y	Y	N	N
1.55/1.64	Amino derivative + glutathione + H_2O	4	554.20	1	Y	Y	N	N
			277.60	2	Y	Y	N	N
1.76/1.93/2.31	Amino derivative + cysteine	9	350.13	1	Y	Y	NN	NN
1.34	Amino derivative + ovothiol A	12 or 14	430.17	1	Y	Y	N	N
			215.58	2	Y	Y	N	N
3.8	Possible benznidazole adduct	26	385.18	1	Y	Y	N	N
1.63	Possible benznidazole adduct	28	368.12	1	N	Y	N	N
3.64/3.8	Possible benznidazole adduct	NA	614.35	1	Y	Y	N	N
2.13	Possible benznidazole metabolite	NA	204.05	1	Y	Y	N	N

Abbreviations: NA, not applicable.
[1]The metabolite numbers refer to the metabolite list in Trochine et al. [10].

Comparative kinetics of trypanosomatid AKRs

The enzymatic properties of the three additional purified homologues were assessed with the same substrates tested against *TcAKR*, finding that all of the trypanosomatid enzymes were capable of using the same substrates (Table 3). Similar to *Tc*AKR, neither the *Leishmania* nor *T. brucei* enzymes were capable of using the nitro-drugs benznidazole or nifurtimox as substrates. As the homologues displayed identical substrate usage, the basic kinetic parameters of each enzyme for each of the substrates were determined at a fixed concentration of NADPH (Table 5). Comparing the apparent K_m^{app} values, substrate turnover rates and catalytic efficiencies of the enzymes revealed *Li*PGFS1 to be more kinetically similar to the *Tc*AKR than *Tb*PGFS, with the opposite relationship true of *Li*PGFS2 suggesting a divergence in AKR evolution in *Leishmania*. We observed the catalytic efficiency (k_{cat}/K_m) of methylglyoxal as a substrate of these enzymes to be relatively unchanged despite up to 20- and 80-fold differences k_{cat} and K_m values, respectively. This trend also was observed for glyoxal, phenylglyoxal and D,L-glyceraldehyde. However, the nitro-aromatic compounds were much more efficiently utilised in the case of *Tb*PGFS or *Li*PGFS2 compared with *Li*PGFS1 and *Tc*AKR. *Li*PGFS2 used in our study appears to be the same as a glutathione-specific aldose reductase [31]; however, it appears that glutathione is not required for the functional activity of this enzyme in our hands. The human prostaglandin $F_{2\alpha}$ synthase (NP_003730.4) also displayed trace activity with methylglyoxal as a substrate, but with a much lower efficiency (~10 M^{-1} s^{-1}), indicating that it is unlikely to be a functional mechanism for detoxification of methylglyoxal in human cells.

Arachidonic acid and prostaglandins

Previous studies on these enzymes have suggested that the *T. brucei* and *Leishmania* spp. AKRs function as prostaglandin $F_{2\alpha}$ synthases in these parasites, converting prostaglandin H_2 (PGH_2) to the $F_{2\alpha}$ form. While our observations for prostaglandin $F_{2\alpha}$ synthase activity of *Tb*PGFS and *Li*PGFS2 were in agreement with the literature [19,20], we also observed $PGF_{2\alpha}$ activity for *Li*PGFS1 (Table 6). We also confirm the lack of prostaglandin $F_{2\alpha}$ synthase activity of *Tc*AKR as reported by Garavaglia et al. [21].

Biochemical Journal (2018) **475** 2593–2610
https://doi.org/10.1042/BCJ20180232

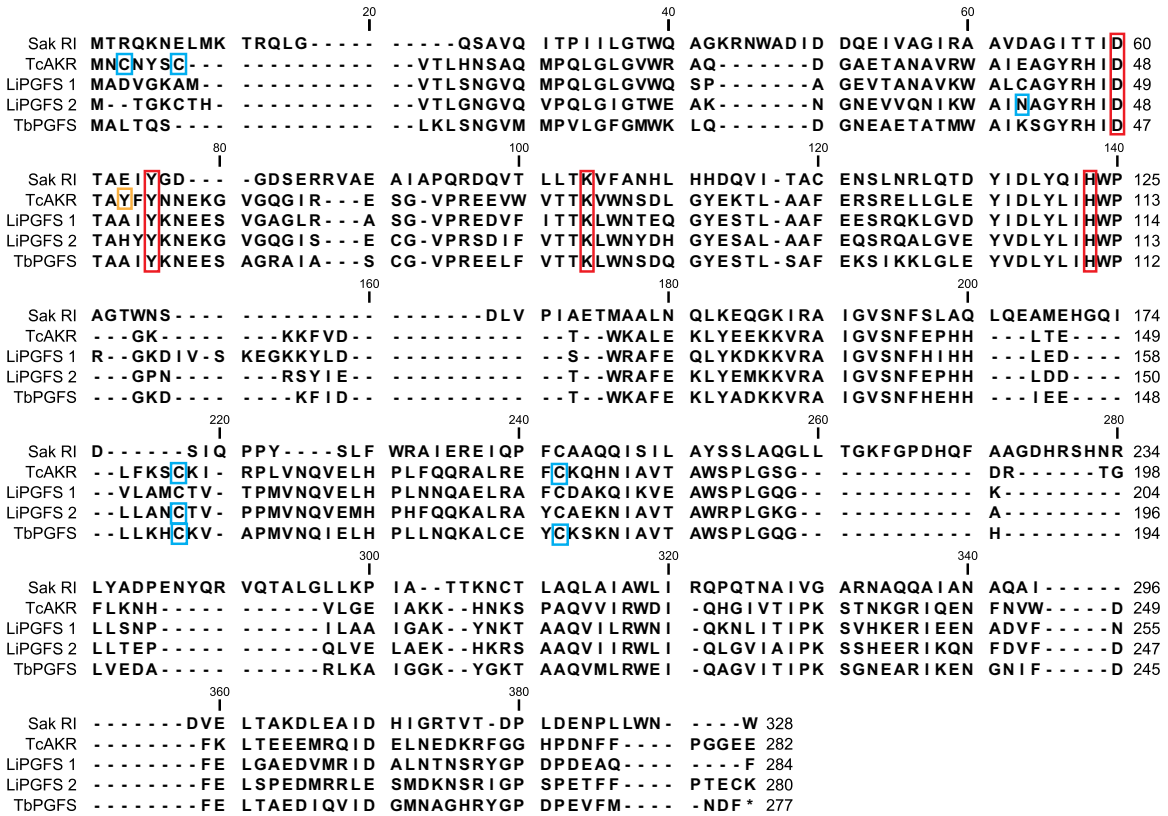

Figure 4. Sequence alignment of AKR homologues identified by BLAST.

Multiple sequence alignment of SakRI, *Tc*AKR (TcCLB.511287.49), *Li*PGFS1 (LinJ.31.2210), *Li*PGFS2 (LinJ.32.0470) and *Tb*PGFS (Tb927.11.4700). The conserved AKR catalytic tetrad identified in *T. brucei* is marked by the red boxes. Blue boxes indicate solvent accessible cysteine residues identified in the crystal structures of *Tb*PGFS *Tc*AKR and *Li*PGFS2 (PDB accession numbers 1VBJ, 4GIE and 4G5D) [27]. Orange box highlighting Y51C allelic variation was observed in CL-Brener.

Observations that these parasites are capable of synthesising PGH_2 from arachidonic acid currently do not fit with the known prostaglandin biosynthetic pathway due to the absence of cyclooxygenases 1 and 2 that catalyse the conversion of arachidonic acid to PGH_2. Our alternative hypothesis is that the formation of the prostaglandins from arachidonic acid could be due to the formation of structurally similar isomers, the isoprostanes. These molecules have been reported as a marker of oxidative stress [34] and are formed by the free radical-mediated peroxidation of arachidonic acid within the cell [35]. In contrast with enzyme-mediated peroxidation that typically generates a single enantiomer of a single regioisomer, non-enzymatic peroxidation generates racemic mixtures with multiple regio- and stereo-centres [36,37]. Among other products, non-enzymatic peroxidation of arachidonic acid produces four F_2-isoprostane regioisomers (Figure 6), each of which comprises eight racemic diastereomers, making 64 in total [38]. Prostaglandin $F_{2\alpha}$ and its isoprostane 8-isoprostane $F_{2\alpha}$ (15-F2t-IsoP or $iPF_{2\alpha}$-III) belong to the 15-series regioisomers, which, together with the 5-series, are formed in greater amounts than the less stable 8- and 12-series [38]. Although the four F_2-isoprostane classes are isobaric (*m*/*z* 353), they can be distinguished by their MRM spectra which yield different fragmentation patterns below *m*/*z* 200, with the 15-series ($iPF_{2\alpha}$-III series) producing a predominant 193 anion [39]. The 5-series produces a minor peak at 193, but can be distinguished by its predominant MRM product at *m*/*z* 115 and different retention time on HPLC. To determine if prostaglandins or isoprostanes could be produced, parasites were co-incubated with arachidonic acid and analysed by LC–MS/MS and compared with known analytical standards. Despite the high sensitivity of the LC–MS/MS assay (LOD of ~0.1 ng ml^{-1} for both species) our initial experiments, where 66 μM arachidonic acid was co-incubated with intact parasites, failed to detect either prostaglandin $F_{2\alpha}$ or its isoprostane 8-isoprostane $F_{2\alpha}$. However, the addition of 1 mM arachidonic acid to hypotonic lysates of *T. brucei* or *T. cruzi* led to the production of multiple isomeric peaks on the MRM channel for

Biochemical Journal (2018) **475** 2593–2610
https://doi.org/10.1042/BCJ20180232

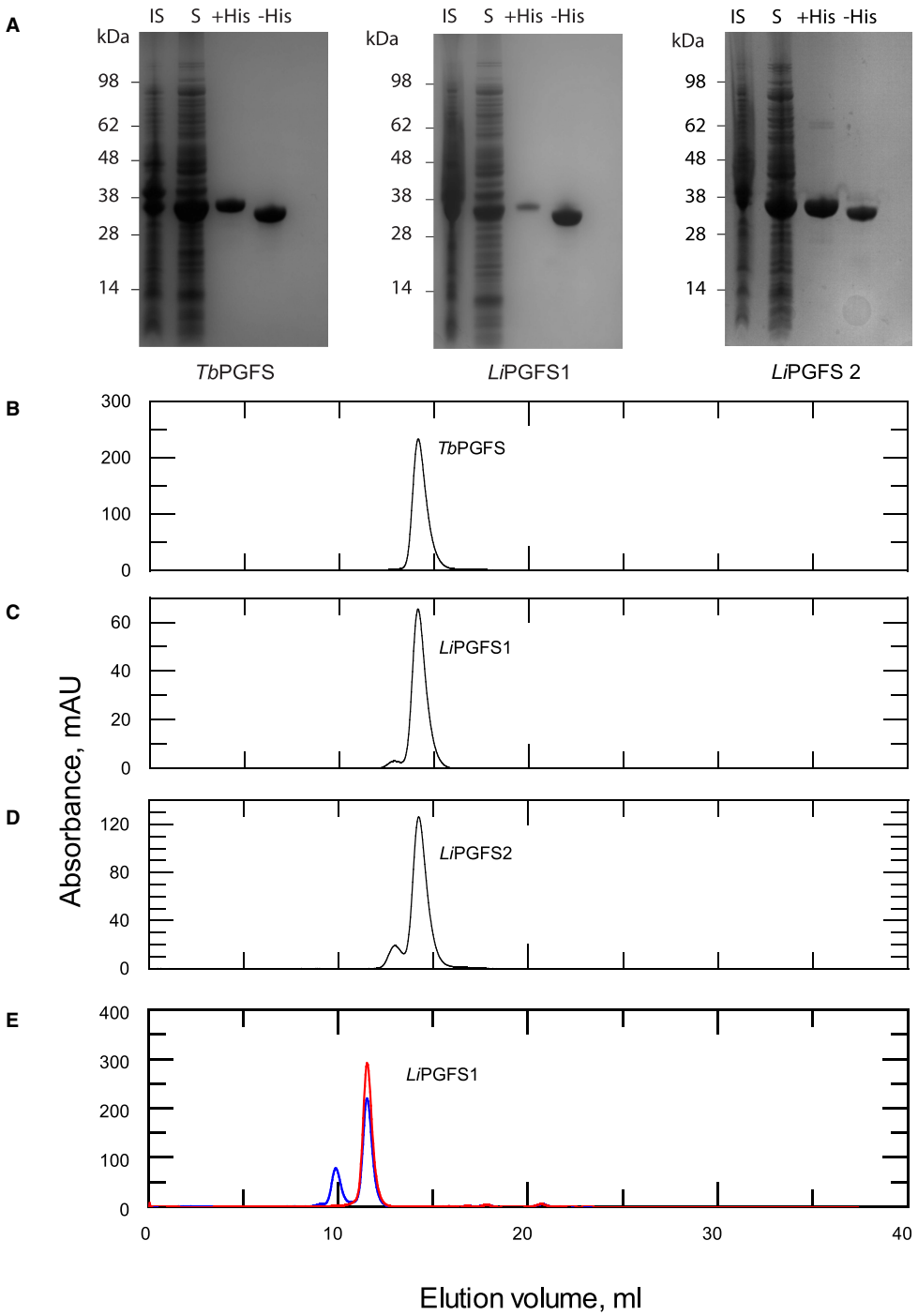

Figure 5. Characterisation of *Li*PGFS1, *Li*PGFS2 and *Tb*PGFS.

(**A**) SDS–PAGE showing purification of *Tb*PGFS1, *Li*PGFS1 and *Li*PGFS2 showing insoluble, soluble, pooled protein from HisTrap column and protein with the hexahistidine tag removed. Size exclusion elution profiles of (**B**) *Tb*PGFS, (**C**) *Li*PGFS1 and (**D**) *Li*PGFS2. Samples were separated on a Superose 12 10/300 column in 25 mM HEPES, 150 mM NaCl, pH 7.33. (**E**) LiPGFS1 stored in the absence of a reducing agent analysed by size exclusion chromatography in the absence (blue) and presence (red) of 0.5 mM TCEP using a Superdex 75 10/300 column.

Biochemical Journal (2018) **475** 2593–2610
https://doi.org/10.1042/BCJ20180232

Table 5 Kinetic characterisation of trypanosomatid recombinant aldo-keto reductases with various substrates

Substrate	Units	*Tc*AKR	*Li*PGFS1	*Li*PGFS2	*Tb*PGFS
Glyoxal					
k_{cat}	s^{-1}	4.56 ± 0.05	7.31 ± 0.19	1.05 ± 0.02	ND
K_m^{app}[1]	mM	8.30 ± 0.31	36.1 ± 2.39	0.56 ± 0.05	ND
k_{cat}/K_m^{app}	M^{-1} s^{-1}	549	202	1880	ND
Methylglyoxal					
k_{cat}	s^{-1}	4.69 ± 0.03	8.72 ± 0.17	1.13 ± <0.01	0.38 ± 0.007
K_m^{app}	mM	0.24 ± <0.001	0.80 ± 0.07	0.02 ± <0.001	0.01 ± <0.001
k_{cat}/K_m^{app}	M^{-1} s^{-1}	19 500	10 900	56 500	38 000
Phenylglyoxal					
k_{cat}	s^{-1}	4.46 ± 0.08	10.4 ± 0.22	1.17 ± 0.02	0.34 ± 0.014
K_m^{app}	mM	0.05 ± 0.003	0.14 ± 0.008	0.01 ± 0.0009	0.005 ± 0.0008
k_{cat}/K_m^{app}	M^{-1} s^{-1}	89 200	74 300	58 500	68 000
2-Nitrobenzaldehyde					
k_{cat}	s^{-1}	2.25 ± 0.11[2]	8.50 ± 0.21	1.04 ± 0.02	0.41 ± 0.002
K_m^{app}	mM	0.71 ± 0.08[2]	0.32 ± 0.02	0.0024 ± 0.0003	0.003 ± 0.0003
k_{cat}/K_m^{app}	M^{-1} s^{-1}	3170	26 600	433 000	140 000
3-Nitrobenzaldehyde					
k_{cat}	s^{-1}	4.07 ± 0.17	1.28 ± 0.03	1.04 ± 0.02	0.34 ± 0.005
K_m^{app}	mM	2.20 ± 0.16	1.55 ± 0.06	0.002 ± 0.0003	0.002 ± 0.0001
k_{cat}/K_m^{app}	M^{-1} s^{-1}	1850	830	520 000	170 000
4-Nitrobenzaldehyde					
k_{cat}	s^{-1}	3.7 ± 0.15	0.48 ± 0.01	1.13 ± 0.05[2]	0.43 ± 0.008
K_m^{app}	mM	68 ± 0.07	0.43 ± 0.026	0.004 ± 0.0006[2]	0.0043 ± 0.0002
k_{cat}/K_m^{app}	M^{-1} s^{-1}	5440	1 110	283 000	100 000
D,L-glyceraldehyde					
k_{cat}	s^{-1}	4.94 ± 0.11	8.72 ± 0.11[2]	2.46 ± 0.13[2]	0.37 ± 0.009
K_m^{app}	mM	1.50 ± 0.17	2.87 ± 0.08[2]	1.07 ± 0.15[2]	0.07 ± 0.005
k_{cat}/K_m^{app}	M^{-1} s^{-1}	3290	3040	2300	5290

Abbreviations: ND, not determined.
[1]K_m^{app} values determined with 100 μM NADPH.
[2]Weighted mean of two individual replicates, all others are $n \geq 3$.

$PGF_{2\alpha}$ and iso-$PGF_{2\alpha}$ (Figure 7). A clearly resolved peak was detected for iso-$PGF_{2\alpha}$, along with a shoulder with the same retention time as $PGF_{2\alpha}$. The identity of the other peaks is not known, but is likely to include the other racemic diastereoisomers in the 15-series (Figure 6). Similar results were obtained for both *T. brucei* and *T. cruzi*.

Discussion

The primary aim of the present study was to assess the capability of *Tc*AKR to reduce or bio-activate clinically relevant monocyclic and bicyclic nitro-drugs that are either in clinical use or under development for the treatment of Chagas disease. Garavaglia et al. [16] reported that recombinant *Tc*AKR and native *Tc*AKR purified from *T. cruzi* epimastigotes were able to reduce benznidazole with specific activities of 0.091 and 0.073 U mg^{-1}, respectively. In complete contrast, we found no evidence for the reduction of benznidazole by *Tc*AKR

Biochemical Journal (2018) **475** 2593–2610
https://doi.org/10.1042/BCJ20180232

Table 6 Identification of prostaglandin $F_{2\alpha}$ synthase activity in trypanosomatid aldo-keto reductases and old yellow enzyme

	Peak area			
Enzyme	**$PGF_{2\alpha}$**	**$PGF_{1\alpha}$**	**PGE_2**	**PGE_1**
No enzyme control	3185		176 250	984
*Hs*PGFS	6415		187 319	537
*Tc*AKR	4231		190 097	1161
*Li*PGFS1	33 807	536	156 739	393
*Li*PGFS2	38 285	467	149 112	273
*Tb*PGFS	28 568	306	139 483	606
*Tc*OYE	25 216	510	133 298	353

Enzymes were incubated with PGH_2 as described in Experimental Procedures and analysed by LC–MS. 6-Keto-$PGF_{2\alpha}$ and iso-$PGF_{2\alpha}$ were not detected. PGH_2 is unstable and in the absence of enzyme is spontaneously rearranged to PGE_2 [32,33].

(<0.001 U mg^{-1}) (Table 3); neither could we detect metabolism of benznidazole by *Tc*AKR using UPLC-QToF/MS under conditions where extensive metabolism occurred in whole cell lysates (Figure 3 and Table 4). It is unlikely that amino acid substitutions in these AKRs are responsible for the discrepancy, because the CL-Brener and Silvio enzymes are 97% identical and molecular modelling shows that the active sites are identical. Differences in assay conditions could be a possible explanation: our assays were at pH 7.33 in HEPES buffer, whereas Garavaglia et al. used Tris–HCl, pH 6.5—an inappropriate buffer system since the pK_a for Tris is 8.3. Notably, these authors reported difficulties in measuring catalytic activity because of non-enzymatic reaction between benznidazole and NADPH cofactor under their experimental conditions. We did not encounter any such problem when pure recombinant *Tc*AKR was assayed under our conditions by spectrophotometry (Figure 2) or by mass spectrometry (Table 4). We conclude that *Tc*AKR is not involved in the bioactivation of benznidazole, but instead we offer a potential role for TcAKR in resistance to benznidazole as discussed below.

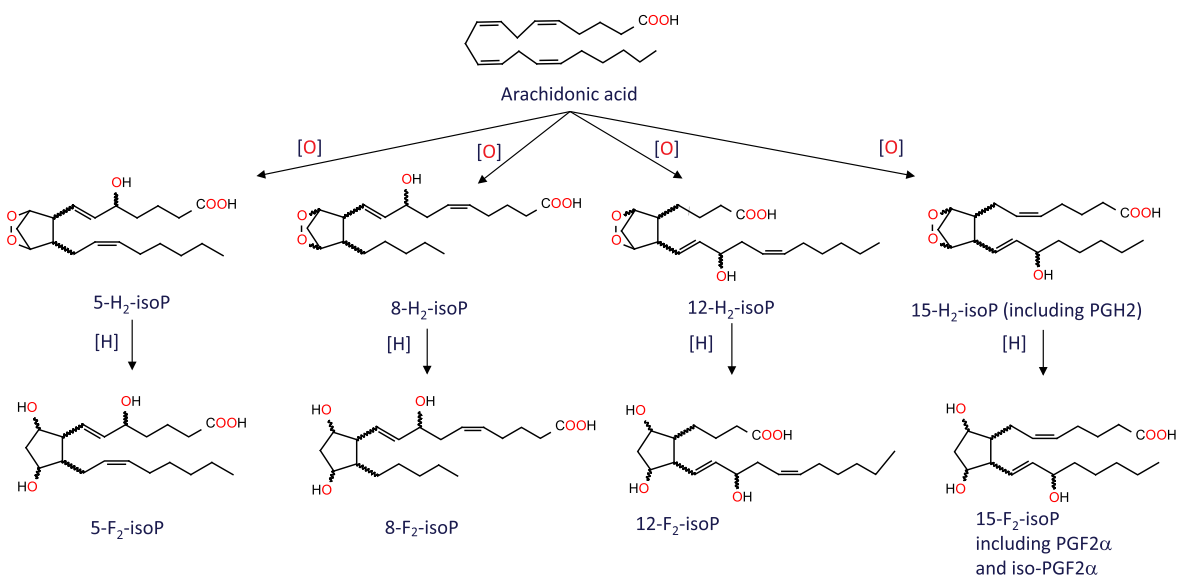

Figure 6. Formation of F_2-isoprostanes from arachidonic acid.
Abbreviations: IsoP, isoprostane.

Biochemical Journal (2018) **475** 2593–2610
https://doi.org/10.1042/BCJ20180232

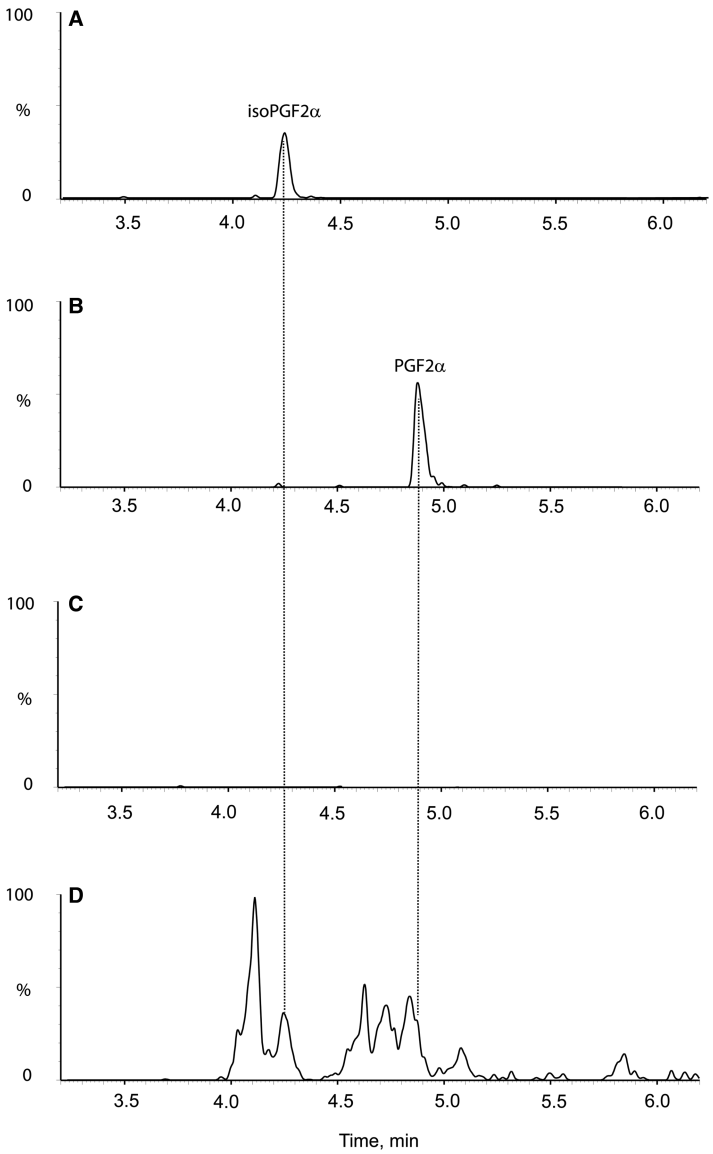

Figure 7. MRM chromatograms monitoring for PGF2α /Iso-PGF2α in *T. cruzi* cell lysates.
Elution profile of 2 ng ml^{-1} standards of iso-PGF2α (**A**) and PDF2α (**B**). *T. cruzi* cell lysates incubated with (**D**) or without (**C**) 1 mM arachidonic acid.

A second aim of our study was to elucidate the possible metabolic functions of these AKR homologues across the Trypanosomatidae. All four enzymes across three representative species possess activity with ketoaldehydes with specificity constants (k_{cat}/K_m) in the order phenylglyoxal > methylglyoxal > glyoxal. Notably, all four enzymes had specificity constants for methylglyoxal (range 1.1–5.7 [$\times 10^4$] M s^{-1}) that are similar to that of SakRI (1.1×10^4 M^{-1} s^{-1}), a bacterial enzyme that has been implicated in methylglyoxal metabolism [18]. The specificity constant for *Tb*PGFS with methylglyoxal (3.8×10^4 M^{-1} s^{-1}) is an order of magnitude lower than that reported with PGH_2 (7×10^5 M^{-1} s^{-1}) [30], whereas the reverse is observed for *Li*PGFS2 with methylglyoxal (5.7×10^4 M^{-1} s^{-1}) preferred over PGH_2 (8.8×10^3 M^{-1} s^{-1}) [20]. As previously reported [21] and confirmed here, the *T. cruzi* enzyme lacks prostaglandin F synthase activity; this is provided instead by old yellow enzyme [32], a protein that is absent in *T. brucei* and *L. infantum*. Given the broad spectrum of activity with ketoaldehydes, aromatic aldehydes, erythroses (the present study) and quinones [16,19,40], these enzymes are more like carbonyl reductases (EC 1.11.184) [41] than prostaglandin F synthases (EC 1.1.1.188). Of the

Biochemical Journal (2018) **475** 2593–2610
https://doi.org/10.1042/BCJ20180232

physiologically relevant substrates examined here, methylglyoxal is a more efficient substrate for all of these enzymes compared with D,L-glyceraldehyde or glyoxal. Enzymes typically operate in cells at substrate concentrations near to or within 10-fold below their K_m [42,43]. Although the concentration of methylglyoxal is not known for these parasites, the K_m^{app} values (0.01–0.8 mM) for methylglyoxal determined here are consistent with physiological levels of free metabolite of <5 μM reported in other cells [44]. The K_m values are thus consistent with a role in defence against carbonyl stress and are at the lower range of K_m values reported for broad specificity methylglyoxal reductases from *Aspergillus* (1.43 and 15.4 mM) [45], *Saccharomyces* (5.9 mM) [46], *Kluyveromyces* (0.43 and 1.6 mM) [47] and *Synechococcus* sp. (0.08 mM) [18].

Our results suggest an important biological role in the detoxification of toxic ketoaldehydes typified by methylglyoxal, formed as a by-product of the glycolytic pathway, as well as from threonine degradation and from lipid peroxidation [48,49]. Our previous studies have identified two pathways for degradation of methylglyoxal in trypanosomatids, either by conversion to D-lactate catalysed by trypanothione-dependent glyoxalases GLO1 and GLO2, or by conversion to L-lactate via methylglyoxal reductase and lactaldehyde dehydrogenase [25]. Methylglyoxal is formed mainly from triose phosphate intermediates in glycolysis, a pathway whose first nine steps, including isomerisation of dihydroxyacetone phosphate and glyceraldehyde 3-phosphate, take place in a peroxisome-like organelle, the glycosome [50]. It is of interest to note that PGFS and GLO2 are present in highly purified glycosomal preparations from *T. brucei* [51] and, likewise, PGFS, GLO1 and two putative D-lactate dehydrogenases are found in *L. donovani* glycosomes [52], suggesting a role for both pathways in protection against protein glycation [48] in these organelles as well as in the cytosol. Curiously, bloodstream forms of *T. brucei* have the highest glycolytic flux of all these trypanosomatids [53], yet lack GLO1 of the trypanothione-dependent glyoxalase pathway present in *Leishmania* spp. and *T. cruzi* [25].

In the case of *Tc*AKR, overexpression of this enzyme confers a modest resistance to benznidazole [16]. Benznidazole is a prodrug and undergoes activation via two sequential two-electron reduction steps by a mitochondrial nitroreductase to form a toxic reactive hydroxylamine intermediate (Figure 8). This compound subsequently forms adducts with low molecular mass thiols [10] or undergoes rearrangement to a

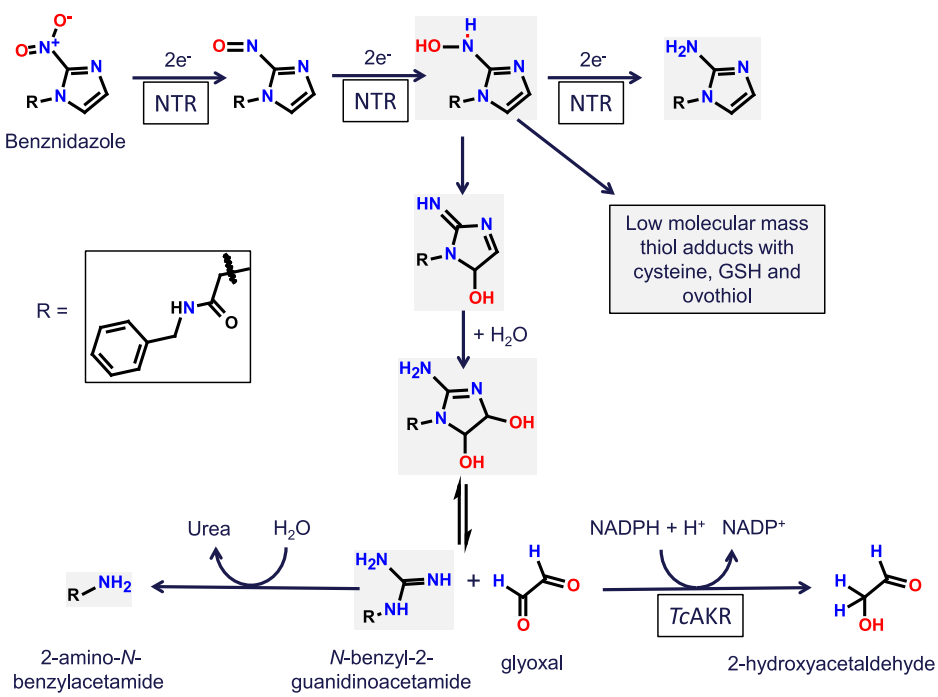

Figure 8. Possible role of AKR in the metabolism of benznidazole.

The metabolites shaded in grey were identified in our study (Table 4). The removal of glyoxal by AKR promotes further metabolism to 2-amino-*N*-benzyl acetamide.

dihydro-dihydroxy intermediate [8] that can dissociate to form glyoxal and *N*-benzyl-2-guanidinoacetamide [54] (Figure 8). Glyoxal is toxic and mutagenic and reacts with DNA to form a cyclic glyoxal-deoxyguanosine adduct, as well as causing deamination of deoxycytidine and cross-linking in DNA [55]. Thus, overexpression of *Tc*AKR may contribute to benznidazole resistance by facilitating removal of glyoxal.

Given the absence of genetic and biochemical evidence for cyclooxygenase-dependent synthesis of PGH_2 from arachidonic acid [19,20,32], the evidence for specific prostaglandin metabolism requires critical reassessment. In mammalian tissues, non-cyclooxygenase-derived F_2-isoprostanes can be formed *in situ* on arachidonic acid-containing phospholipids via lipid peroxidation and then released by the action of phospholipase A_2 [35]. Alternatively, they can be formed from free arachidonic acid *in vitro* [56]. *Leishmania* spp. are able to synthesise arachidonic acid *de novo* [57], whereas *T. cruzi* and *T. brucei* are able to scavenge it from the extracellular medium and incorporate it into lipid bodies [57–59]. All species contain phospholipase A_2 [60,61]. Our findings support the non-enzymatic formation of PGH_2 and other F-type isoprostanes by free radical peroxidation of arachidonic acid. Notably, the formation of multiple isobaric products (*m*/*z* 353) with the characteristic MRM signal for the 15-series of F-type prostanoids (*m*/*z* 193) supports a non-enzymatic peroxidation mechanism, in contrast with a cyclooxygenase-catalysed peroxidation that would generate a single enantiomerically pure product [36,37]. In this respect, it is worth noting that the four studies reporting enzymatic conversion of arachidonic acid into PGD_2, PGE_2 and $PGF_{2\alpha}$ utilised an analytical approach that focuses exclusively on these prostanoids [19,32,40,59] and predates the discovery of isoprostanes. The method involves incubation of whole cell lysates with saturating amounts of arachidonic acid, spiking with trace amounts of radiolabelled PGD_2, PGE_2 and $PGF_{2\alpha}$, separation by HPLC and quantitation of radiolabelled peaks by enzyme immunoassay [62]. Thus, the large number of additional F_2-isoprostane metabolites observed here (Figure 7) may have been missed. We propose that arachidonic acid (free or as phospholipid) undergoes non-enzymatic peroxidation to form 8-iso-PGH_2 (among other enantiomers) which serves as a substrate for AKRs to form 8-iso-$PGF_{2\alpha}$ (and other isoprostanes). Additionally, we note that a report that *T. cruzi* produces thromboxane A_2 as well as $PGF_{2\alpha}$ [63] could also involve a non-enzymatic pathway [64]. Thus, there is a need for a thorough re-evaluation of the nature of eicosanoids formed in these parasites and the possible physiological role of the products. For example, it is worth noting that host immune responses to parasite infection often involve oxidant stress [65,66] and that certain prostanoids formed via the free radical route can have biological activity [67].

In conclusion, we have demonstrated that the substrate-specificity of these aldo-keto reductases is broader than other prostaglandin $F_{2\alpha}$ synthases and that they are likely to be involved in the elimination of certain toxic ketoaldehyde metabolites derived from lipids, trioses and the drug, benznidazole.

Abbreviations

AKR, aldo-keto reductase; MRM, multiple reaction monitoring; NTR, nitroreductase; ORFs, open reading frames; PGF2α, prostaglandin $F_{2\alpha}$; PGH_2, prostaglandin H.

Author Contribution

A.H.F. conceived the project. A.J.R., S.N., P.S. and A.H.F. designed the experiments. A.J.R., J.D., S.N. and P.S. performed the experiments. All authors analysed the data and contributed to the manuscript.

Funding

This work was supported by a grant from the Welcome Trust [079838] with additional co-funding from the Wellcome Trust/Bill and Melinda Gates Foundation [OPP1066891]. J.D. was supported by a James Black prize studentship funded by the University of Dundee.

Acknowledgements

We thank the DNA sequencing service at the University of Dundee and the Ferguson group for the use of their Superose 12 column.

Competing Interests

The Authors declare that there are no competing interests associated with the manuscript.

Biochemical Journal (2018) **475** 2593–2610
https://doi.org/10.1042/BCJ20180232

References

1 Stuart, K., Brun, R., Croft, S., Fairlamb, A., Gürtler, R.E., McKerrow, J. et al. (2008) Kinetoplastids: related protozoan pathogens, different diseases. *J. Clin. Invest.* **118**, 1301–1310 https://doi.org/10.1172/JCI33945

2 Feasey, N., Wansbrough-Jones, M., Mabey, D.C.W. and Solomon, A.W. (2010) Neglected tropical diseases. *Br. Med. Bull.* **93**, 179–200 https://doi.org/10.1093/bmb/ldp046

3 Eperon, G., Balasegaram, M., Potet, J., Mowbray, C., Valverde, O. and Chappuis, F. (2014) Treatment options for second-stage gambiense human African trypanosomiasis. *Expert Rev. Anti. Infect. Ther.* **12**, 1407–1417 https://doi.org/10.1586/14787210.2014.959496

4 Bahia, M.T., de Andrade, I.M., Martins, T.A.F., da Silva do Nascimento, A.F., Diniz, L.F., Caldas, I.S. et al. (2012) Fexinidazole: a potential new drug candidate for Chagas disease. *PLoS Negl. Trop. Dis.* **6**, e1870 https://doi.org/10.1371/journal.pntd.0001870

5 Wyllie, S., Patterson, S., Stojanovski, L., Simeons, F.R.C., Norval, S., Kime, R. et al. (2012) The anti-trypanosome drug fexinidazole shows potential for treating visceral leishmaniasis. *Sci. Transl. Med.* **4**, 119re1 https://doi.org/10.1126/scitranslmed.3003326

6 Kaiser, M., Bray, M.A., Cal, M., Bourdin Trunz, B., Torreele, E. and Brun, R. (2011) Antitrypanosomal activity of fexinidazole, a new oral nitroimidazole drug candidate for treatment of sleeping sickness. *Antimicrob. Agents Chemother.* **55**, 5602–5608 https://doi.org/10.1128/AAC.00246-11

7 Wilkinson, S.R., Taylor, M.C., Horn, D., Kelly, J.M. and Cheeseman, I. (2008) A mechanism for cross-resistance to nifurtimox and benznidazole in trypanosomes. *Proc. Natl Acad. Sci. U.S.A.* **105**, 5022–5027 https://doi.org/10.1073/pnas.0711014105

8 Hall, B.S. and Wilkinson, S.R. (2012) Activation of benznidazole by trypanosomal type I nitroreductases results in glyoxal formation. *Antimicrob. Agents Chemother.* **56**, 115–123 https://doi.org/10.1128/AAC.05135-11

9 Hall, B.S., Bot, C. and Wilkinson, S.R. (2011) Nifurtimox activation by trypanosomal type I nitroreductases generates cytotoxic nitrile metabolites. *J. Biol. Chem.* **286**, 13088–13095 https://doi.org/10.1074/jbc.M111.230847

10 Trochine, A., Creek, D.J., Faral-Tello, P., Barrett, M.P. and Robello, C. (2014) Benznidazole biotransformation and multiple targets in *Trypanosoma cruzi* revealed by metabolomics. *PLoS Negl. Trop. Dis.* **8**, e2844 https://doi.org/10.1371/journal.pntd.0002844

11 Wyllie, S., Foth, B.J., Kelner, A., Sokolova, A.Y., Berriman, M. and Fairlamb, A.H. (2016) Nitroheterocyclic drug resistance mechanisms in *Trypanosoma brucei*. *J. Antimicrob. Chemother.* **71**, 625–634 https://doi.org/10.1093/jac/dkv376

12 Sokolova, A.Y., Wyllie, S., Patterson, S., Oza, S.L., Read, K.D. and Fairlamb, A.H. (2010) Cross-resistance to nitro drugs and implications for treatment of human African trypanosomiasis. *Antimicrob. Agents Chemother.* **54**, 2893–2900 https://doi.org/10.1128/AAC.00332-10

13 Andrade, H.M., Murta, S.M.F., Chapeaurouge, A., Perales, J., Nirdé, P. and Romanha, A.J. (2008) Proteomic analysis of *Trypanosoma cruzi* resistance to benznidazole. *J. Proteome Res.* **7**, 2357–2367 https://doi.org/10.1021/pr700659m

14 Murta, S.M.F., Krieger, M.A., Montenegro, L.R., Campos, F.F.M., Probst, C.M., Ávila, A.R. et al. (2006) Deletion of copies of the gene encoding old yellow enzyme (TcOYE), a NAD(P)H flavin oxidoreductase, associates with in vitro-induced benznidazole resistance in *Trypanosoma cruzi*. *Mol. Biochem. Parasitol.* **146**, 151–162 https://doi.org/10.1016/j.molbiopara.2005.12.001

15 Trochine, A., Alvarez, G., Corre, S., Faral-Tello, P., Durán, R., Batthyany, C.I. et al. (2014) *Trypanosoma cruzi* chemical proteomics using immobilized benznidazole. *Exp. Parasitol.* **140**, 33–38 https://doi.org/10.1016/j.exppara.2014.03.013

16 Garavaglia, P.A., Laverrière, M., Cannata, J.J. and García, G.A. (2016) Putative role of the aldo-keto reductase from *Trypanosoma cruzi* in benznidazole metabolism. *Antimicrob. Agents Chemother.* **60**, 2664–2670 https://doi.org/10.1128/AAC.02185-15

17 Jez, J.M. and Penning, T.M. (2001) The aldo-keto reductase (AKR) superfamily: an update. *Chem. Biol. Interact.* **130–132**, 499–525 https://doi.org/10.1016/S0009-2797(00)00295-7

18 Xu, D., Liu, X., Guo, C., and Zhao, J. (2006) Methylglyoxal detoxification by an aldo-keto reductase in the cyanobacterium *Synechococcus* sp. PCC 7002. *Microbiology* **152**, 2013–2021 https://doi.org/10.1099/mic.0.28870-0

19 Kubata, B.K., Duszenko, M., Kabututu, Z., Rawer, M., Szallies, A., Fujimori, K. et al. (2000) Identification of a novel prostaglandin F_{2a} synthase in *Trypanosoma brucei*. *J. Exp. Med.* **192**, 1327–1338 https://doi.org/10.1084/jem.192.9.1327

20 Kabututu, Z., Martin, S.K., Nozaki, T., Kawazu, S.-i., Okada, T., Munday, C.J. et al. (2003) Prostaglandin production from arachidonic acid and evidence for a 9,11-endoperoxide prostaglandin H_2 reductase in *Leishmania*. *Int. J. Parasitol.* **33**, 221–228 https://doi.org/10.1016/S0020-7519(02)00254-0

21 Garavaglia, P.A., Cannata, J.J.B., Ruiz, A.M., Maugeri, D., Duran, R., Galleano, M. et al. (2010) Identification, cloning and characterization of an aldo-keto reductase from *Trypanosoma cruzi* with quinone oxido-reductase activity. *Mol. Biochem. Parasitol.* **173**, 132–141 https://doi.org/10.1016/j.molbiopara.2010.05.019

22 Studier, F.W. (2005) Protein production by auto-induction in high-density shaking cultures. *Protein Exp. Purif.* **41**, 207–234 https://doi.org/10.1016/j.pep.2005.01.016

23 Young, H.D. (1962) *Statistical Treatment of Experimental Data*, McGraw-Hill, New York

24 Hunter, K.J., Le Quesne, S.A. and Fairlamb, A.H. (1994) Identification and biosynthesis of N^1,N^9-*bis*(glutathionyl)aminopropylcadaverine (homotrypanothione) in *Trypanosoma cruzi*. *Eur. J. Biochem.* **226**, 1019–1027 https://doi.org/10.1111/j.1432-1033.1994.t01-1-01019.x

25 Greig, N., Wyllie, S., Patterson, S. and Fairlamb, A.H. (2009) A comparative study of methylglyoxal metabolism in trypanosomatids. *FEBS J.* **276**, 376–386 https://doi.org/10.1111/j.1742-4658.2008.06788.x

26 Goyard, S., Segawa, H., Gordon, J., Showalter, M., Duncan, R., Turco, S.J. et al. (2003) An *in vitro* system for developmental and genetic studies of *Leishmania donovani* phosphoglycans. *Mol. Biochem. Parasitol.* **130**, 31–42 https://doi.org/10.1016/S0166-6851(03)00142-7

27 Moen, S.O., Fairman, J.W., Barnes, S.R., Sullivan, A., Nakazawa-Hewitt, S., Van Voorhis, W.C. et al. (2015) Structures of prostaglandin F synthase from the protozoa *Leishmania major* and *Trypanosoma cruzi* with NADP. *Acta Crystallogr., Sect. F: Struct. Biol. Commun.* **71**, 609–614 https://doi.org/10.1107/S2053230X15006883

28 Patterson, S., Wyllie, S., Stojanovski, L., Perry, M.R., Simeons, F.R.C., Norval, S. et al. (2013) The *R* enantiomer of the anti-tubercular drug PA-824 as a potential oral treatment for visceral leishmaniasis. *Antimicrob. Agents Chemother.* **57**, 4699–4706 https://doi.org/10.1128/AAC.00722-13

29 Wyllie, S. and Fairlamb, A.H. (2011) Methylglyoxal metabolism in trypanosomes and leishmania. *Semin. Cell Dev. Biol.* **22**, 271–277 https://doi.org/10.1016/j.semcdb.2011.02.001

30 Kilunga, K.B., Inoue, T., Okano, Y., Kabututu, Z., Martin, S.K., Lazarus, M. et al. (2005) Structural and mutational analysis of *Trypanosoma brucei* prostaglandin H_2 reductase provides insight into the catalytic mechanism of aldo-ketoreductases. *J. Biol. Chem.* **280**, 26371–26382 https://doi.org/10.1074/jbc.M413884200

31 Rath, J., Gowri, V. S., Chauhan, S. C., Padmanabhan, P. K., Srinivasan, N. and Madhubala, R. (2009) A glutathione-specific aldose reductase of *Leishmania donovani* and its potential implications for methylglyoxal detoxification pathway. *Gene* **429**, 1–9

32 Kubata, B.K., Kabututu, Z., Nozaki, T., Munday, C.J., Fukuzumi, S., Ohkubo, K. et al. (2002) A key role for old yellow enzyme in the metabolism of drugs by *Trypanosoma cruzi*. *J. Exp. Med.* **196**, 1241–1252 https://doi.org/10.1084/jem.20020885

33 Hamberg, M. and Samuelsson, B. (1973) Detection and isolation of an endoperoxide intermediate in prostaglandin biosynthesis. *Proc. Natl Acad. Sci. U.S.A.* **70**, 899–903 https://doi.org/10.1073/pnas.70.3.899

34 Milne, G.L., Yin, H., Brooks, J.D., Sanchez, S., Jackson, R.L. and Morrow, J.D. (2007) Quantification of F_2-isoprostanes in biological fluids and tissues as a measure of oxidant stress. *Methods Enzymol.* **433**, 113–126 https://doi.org/10.1016/S0076-6879(07)33006-1

35 Morrow, J.D., Awad, J.A., Boss, H.J., Blair, I.A. and Roberts, L.J. (1992) Non-cyclooxygenase-derived prostanoids (F_2-isoprostanes) are formed *in situ* on phospholipids. *Proc. Natl Acad. Sci. U.S.A.* **89**, 10721–10725 https://doi.org/10.1073/pnas.89.22.10721

36 Roberts, L.J. and Milne, G.L. (2009) Isoprostanes. *J. Lipid Res.* **50**(Suppl), S219–S223 https://doi.org/10.1194/jlr.R800037-JLR200

37 Davies, S.S. and Guo, L. (2014) Lipid peroxidation generates biologically active phospholipids including oxidatively *N*-modified phospholipids. *Chem. Phys. Lipids* **181**, 1–33 https://doi.org/10.1016/j.chemphyslip.2014.03.002

38 Milne, G.L., Dai, Q. and Roberts, L.J. (2015) The isoprostanes—25 years later. *Biochim. Biophys. Acta, Mol. Cell Biol. Lipids* **1851**, 433–445 https://doi.org/10.1016/j.bbalip.2014.10.007

39 Li, H., Lawson, J.A., Reilly, M., Adiyaman, M., Hwang, S.-W., Rokach, J. et al. (1999) Quantitative high performance liquid chromatography/tandem mass spectrometric analysis of the four classes of F_2-isoprostanes in human urine. *Proc. Natl Acad. Sci. U.S.A.* **96**, 13381–13386 https://doi.org/10.1073/pnas.96.23.13381

40 Kabututu, Z., Martin, S.K., Nozaki, T., Kawazu, S., Okada, T., Munday, C.J. et al. (2002) Prostaglandin production from arachidonic acid and evidence for a 9,11-endoperoxide prostaglandin H2 reductase in *Leishmania*. *Int. J. Parasitol.* **32**, 1693–1700 https://doi.org/10.1016/S0020-7519(02)00160-1

41 Wermuth, B. (1981) Purification and properties of an NADPH-dependent carbonyl reductase from human brain. Relationship to prostaglandin 9-ketoreductase and xenobiotic ketone reductase. *J. Biol. Chem.* **256**, 1206–1213 PMID:7005231

42 Fersht, A.R. (1974) Catalysis, binding and enzyme-substrate complementarity. *Proc. R. Soc. Lond. B Biol. Sci.* **187**, 397–407 https://doi.org/10.1098/rspb.1974.0084

43 Copeland, R.A. (2005) Evaluation of Enzyme Inhibitors in Drug Discovery: A Guide for Medicinal Chemists and Pharmacologists John Wiley & Sons, Hoboken, p. 77

44 Rabbani, N. and Thornalley, P.J. (2014) Measurement of methylglyoxal by stable isotopic dilution analysis LC-MS/MS with corroborative prediction in physiological samples. *Nat. Protoc.* **9**, 1969–1979 https://doi.org/10.1038/nprot.2014.129

45 Inoue, Y., Rhee, H.-i., Watanabe, K., Murata, K. and Kimura, A. (1988) Metabolism of 2-oxoaldehyde in mold. Purification and characterization of two methylglyoxal reductases from *Aspergillus niger*. *Eur. J. Biochem.* **171**, 213–218 https://doi.org/10.1111/j.1432-1033.1988.tb13778.x

46 Murata, K., Fukuda, Y., Simosaka, M., Watanabe, K., Saikusa, T. and Kimura, A. (1985) Metabolism of 2-oxoaldehyde in yeasts. Purification and characterization of NADPH-dependent methylglyoxal-reducing enzyme from *Saccharomyces cerevisiae*. *Eur. J. Biochem.* **151**, 631–636 https://doi.org/10.1111/j.1432-1033.1985.tb09151.x

47 Akita, H., Watanabe, M., Suzuki, T., Nakashima, N. and Hoshino, T. (2015) Molecular cloning and characterization of two *YGL039w* genes encoding broad specificity NADPH-dependent aldehyde reductases from *Kluyveromyces marxianus* strain DMB1. *FEMS Microbiol. Lett.* **362**, fnv116 https://doi.org/10.1093/femsle/fnv116

48 Thornalley, P.J. (1996) Pharmacology of methylglyoxal: formation, modification of proteins and nucleic acids, and enzymatic detoxification — a role in pathogenesis and antiproliferative chemotherapy. *Gen. Pharmacol.* **27**, 565–573 https://doi.org/10.1016/0306-3623(95)02054-3

49 Chakraborty, S., Karmakar, K. and Chakravortty, D. (2014) Cells producing their own nemesis: understanding methylglyoxal metabolism. *IUBMB. Life* **66**, 667–678 https://doi.org/10.1002/iub.1324

50 Opperdoes, F.R. (1984) Localization of the initial steps in alkoxyphospholipid biosynthesis in glycosomes (microbodies) of *Trypanosoma brucei*. *FEBS Lett.* **169**, 35–39 https://doi.org/10.1016/0014-5793(84)80284-7

51 Güther, M.L.S., Urbaniak, M.D., Tavendale, A., Prescott, A. and Ferguson, M.A.J. (2014) High-confidence glycosome proteome for procyclic form *Trypanosoma brucei* by epitope-tag organelle enrichment and SILAC proteomics. *J. Proteome Res.* **13**, 2796–2806 https://doi.org/10.1021/pr401209w

52 Jamdhade, M.D., Pawar, H., Chavan, S., Sathe, G., Umasankar, P.K., Mahale, K.N. et al. (2015) Comprehensive proteomics analysis of glycosomes from *Leishmania donovani*. *OMICS* **19**, 157–170 https://doi.org/10.1089/omi.2014.0163

53 Fairlamb, A.H. and Opperdoes, F. R. (1986) Carbohydrate metabolism in African trypanosomes, with special reference to the glycosome In *Carbohydrate Metabolism in Cultured Cells* (Morgan, M.J., ed.), pp. 183–224, Plenum Publishing Corporation, New York

54 Panicucci, R. and McClelland, R.A. (1989) 4,5-Dihydro-4,5-dihydroxyimidazoles as products of the reduction of 2-nitroimidazoles. HPLC assay and demonstration of equilibrium transfer of glyoxal to guanine. *Can. J. Chem.* **67**, 2128–2135 https://doi.org/10.1139/v89-331

55 Kasai, H., Iwamoto-Tanaka, N. and Fukada, S. (1998) DNA modifications by the mutagen glyoxal: adduction to G and C, deamination of C and GC and GA cross-linking. *Carcinogenesis* **19**, 1459–1465 https://doi.org/10.1093/carcin/19.8.1459

56 Morrow, J.D., Harris, T.M. and Roberts, L.J. (1990) Noncyclooxygenase oxidative formation of a series of novel prostaglandins: analytical ramifications for measurement of eicosanoids. *Anal. Biochem.* **184**, 1–10 https://doi.org/10.1016/0003-2697(90)90002-Q

57 Livore, V.I., Tripodi, K.E.J. and Uttaro, A.D. (2007) Elongation of polyunsaturated fatty acids in trypanosomatids. *FEBS J.* **274**, 264–274 https://doi.org/10.1111/j.1742-4658.2006.05581.x

58 Uttaro, A.D. (2014) Acquisition and biosynthesis of saturated and unsaturated fatty acids by trypanosomatids. *Mol. Biochem. Parasitol.* **196**, 61–70 https://doi.org/10.1016/j.molbiopara.2014.04.001

59 Toledo, D.A.M., Roque, N.R., Teixeira, L., Milán-Garcés, E.A., Carneiro, A.B., Almeida, M.R. et al. (2016) Lipid body organelles within the parasite *Trypanosoma cruzi*: a role for intracellular arachidonic acid metabolism. *J. Parasitol. Res.* **11**, e0160433 https://doi.org/10.1371/journal.pone.0160433

60 Ridgley, E.L. and Ruben, L. (2001) Phospholipase from *Trypanosoma brucei* releases arachidonic acid by sequential sn-1, sn-2 deacylation of phospholipids. *Mol. Biochem. Parasitol.* **114**, 29–40 https://doi.org/10.1016/S0166-6851(01)00234-1

61 Catisti, R., Uyemura, S.A., Docampo, R. and Vercesi, A.E. (2000) Calcium mobilization by arachidonic acid in trypanosomatids. *Mol. Biochem. Parasitol.* **105**, 261–271 https://doi.org/10.1016/S0166-6851(99)00186-3

Biochemical Journal (2018) **475** 2593–2610
https://doi.org/10.1042/BCJ20180232

62 Ujihara, M., Urade, Y., Eguchi, N., Hayashi, H., Ikai, K. and Hayaishi, O. (1988) Prostaglandin D2 formation and characterization of its synthetases in various tissues of adult rats. *Arch. Biochem. Biophys.* **260**, 521–531 https://doi.org/10.1016/0003-9861(88)90477-8

63 Ashton, A.W., Mukherjee, S., Nagajyothi, F.N.U., Huang, H., Braunstein, V.L., Desruisseaux, M.S. et al. (2007) Thromboxane A_2 is a key regulator of pathogenesis during *Trypanosoma cruzi* infection. *J. Exp. Med.* **204**, 929–940 https://doi.org/10.1084/jem.20062432

64 Morrow, J.D., Awad, J.A., Wu, A., Zackert, W.E., Daniel, V.C. and Roberts, L.J. (1996) Nonenzymatic free radical-catalyzed generation of thromboxane-like compounds (isothromboxanes) *in vivo*. *J. Biol. Chem.* **271**, 23185–23190 https://doi.org/10.1074/jbc.271.38.23185

65 Turrens, J.F. (2004) Oxidative stress and antioxidant defenses: a target for the treatment of diseases caused by parasitic protozoa. *Mol. Aspects Med.* **25**, 211–220 https://doi.org/10.1016/j.mam.2004.02.021

66 Mauël, J. (1996) Intracellular survival of protozoan parasites with special reference to *Leishmania* spp., *Toxoplasma gondii* and *Trypanosoma cruzi*. *Adv. Parasitol.* **38**, 1–51 https://doi.org/10.1016/S0065-308X(08)60032-9

67 Roberts, L.J., Brame, C.J., Chen, Y. and Morrow, J.D. (1999) Novel eicosanoids. Isoprostanes and related compounds. *Methods Mol. Biol.* **120**, 257–285 https://doi.org/10.1385/1-59259-263-5:257